

BEC Polaron at Finite Momentum 111 TEST

Kushal, Yulia, Eugene

We study the behavior of an impurity immersed in a weakly interacting BEC of ultra-cold atoms. Using the variational approach we study the dynamics of the system after a sudden immersion of the impurity as well as a stationary state that system reaches in long-time limit.

I. MODEL

We study an impurity at finite momentum P immersed in the weakly interacting BEC of ultracold atoms near the inter-species Feshbach resonance. We describe the weakly interacting bosonic gas (with interaction constant g_{BB}) using the Bogoliubov approximation. We expand the bosonic system around macroscopically occupied zero momentum state $a_0 = \sqrt{n_0}$ and introduce Bogoliubov excitations around the condensate. Impurity interact with the the BEC locally, with the parameter of the contact interaction g_Λ ,

$$\begin{aligned} \hat{H} = & \frac{P^2}{2m_I} + \sum_{\mathbf{k}} \omega_{\mathbf{k}} b_{\mathbf{k}}^\dagger b_{\mathbf{k}} \\ & + g_\Lambda n_0 + g_\Lambda \sqrt{n_0} \sum_{\mathbf{k} \neq 0} W_{\mathbf{k}} e^{i\mathbf{k}\mathbf{R}} (b_{-\mathbf{k}}^\dagger + b_{\mathbf{k}}) \\ & + g_\Lambda \sum_{\mathbf{k} \neq 0, \mathbf{k}' \neq 0} V_{\mathbf{k}, \mathbf{k}'}^{(1)} e^{i(\mathbf{k}-\mathbf{k}')\mathbf{R}} b_{\mathbf{k}}^\dagger b_{\mathbf{k}'} \\ & + \frac{1}{2} g_\Lambda \sum_{\mathbf{k} \neq 0, \mathbf{k}' \neq 0} V_{\mathbf{k}, \mathbf{k}'}^{(2)} e^{i(\mathbf{k}-\mathbf{k}')\mathbf{R}} (b_{\mathbf{k}}^\dagger b_{-\mathbf{k}'}^\dagger + b_{-\mathbf{k}} b_{\mathbf{k}'} \end{aligned} \quad (1)$$

Here the operators $b_{\mathbf{k}}^\dagger$ create Bogoliubov quasiparticles ('phonons') with momentum \mathbf{k} and dispersion $\omega_{\mathbf{k}}$. The bare inter-species interaction is given by g_Λ . Furthermore $W_{\mathbf{k}} = \sqrt{\varepsilon_{\mathbf{k}}/\omega_{\mathbf{k}}}$, $V_{\mathbf{k}\mathbf{k}'}^{(1)} \pm V_{\mathbf{k}\mathbf{k}'}^{(2)} = (W_{\mathbf{k}}W_{\mathbf{k}'})^{\pm 1}$, and $\varepsilon_{\mathbf{k}} = k^2/2m_B$ is the boson's dispersion relation; n is the condensate density. We set the system's volume to be one.

We describe the impurity-bath system in the frame co-moving with the polaronic quasiparticle [?]. This is achieved using a canonical transformation $\hat{\mathcal{H}} = \hat{S}^{-1} \hat{H} \hat{S}$ with $\hat{S} = e^{i\hat{\mathbf{R}}\hat{\mathbf{P}}_B}$ where $\hat{\mathbf{P}}_B = \sum_{\mathbf{k}} \mathbf{k} \hat{b}_{\mathbf{k}}^\dagger \hat{b}_{\mathbf{k}}$ is the total momentum operator of the bosons. After the transformation sectors with different total system momentum \mathbf{P} are decoupled in the Hamiltonian $\hat{\mathcal{H}}$. The bosons now interact with each other since the impurity kinetic energy transforms according to $\hat{\mathbf{P}}^2/2M \rightarrow (\hat{\mathbf{P}} - \hat{\mathbf{P}}_B)^2/2M$ [?]. After the Lee-Low-Pines transformation our Hamilto-

nian reads

$$\begin{aligned} \hat{H}_{LLP} = & \frac{1}{2m_I} \left(\mathbf{P} - \sum_{\mathbf{k}} \mathbf{k} \cdot b_{\mathbf{k}}^\dagger b_{\mathbf{k}} \right)^2 + \sum_{\mathbf{k}} \omega_{\mathbf{k}} b_{\mathbf{k}}^\dagger b_{\mathbf{k}} \quad (2) \\ & + g_\Lambda n_0 + g_\Lambda \sqrt{n_0} \sum_{\mathbf{k} \neq 0} W_{\mathbf{k}} (b_{-\mathbf{k}}^\dagger + b_{\mathbf{k}}) \\ & + g_\Lambda \sum_{\mathbf{k} \neq 0, \mathbf{k}' \neq 0} V_{\mathbf{k}, \mathbf{k}'}^{(1)} b_{\mathbf{k}}^\dagger b_{\mathbf{k}'} \\ & + \frac{1}{2} g_\Lambda \sum_{\mathbf{k} \neq 0, \mathbf{k}' \neq 0} V_{\mathbf{k}, \mathbf{k}'}^{(2)} (b_{\mathbf{k}}^\dagger b_{-\mathbf{k}'}^\dagger + b_{-\mathbf{k}} b_{\mathbf{k}'} \end{aligned}$$

We use the variational approach to describe the stationary state of the system as well as a dynamics of the system [?]. We use a trial wavefunction in the form of coherent state [?]

$$|\Psi_{\text{coh}}(t)\rangle = e^{-i\phi(t)} e^{\sum_{\mathbf{k}} \beta_{\mathbf{k}}(t) b_{\mathbf{k}}^\dagger - h.c.} |0\rangle \quad (3)$$

where $\beta_{\mathbf{k}}(t)$ are the coherent amplitudes, $\phi(t)$ is a global phase which ensures energy conservation, and $|0\rangle$ denotes the vacuum of Bogoliubov quasiparticles. We derive the equation of motions for the variational parameters for the variational parameters of the wavefunction, $\frac{d}{dt} \frac{\partial \mathcal{L}}{\partial \beta} - \frac{\partial \mathcal{L}}{\partial \beta} = 0$, from the Lagrangian calculated with respect to our trial state $\mathcal{L} = \langle \Psi_{\text{coh}} | i\partial_t - \hat{\mathcal{H}} | \Psi_{\text{coh}} \rangle$,

$$\begin{aligned} i\dot{\beta}_{\mathbf{k}} = & g_\Lambda \sqrt{n} W_{\mathbf{k}} + \left(\omega_{\mathbf{k}} + \frac{\mathbf{k}^2}{2m_I} - \frac{\mathbf{k}(\mathbf{P} - \mathbf{P}_B[\beta_{\mathbf{k}}])}{m_I} \right) \beta_{\mathbf{k}} \\ & + \frac{g_\Lambda}{2} W_{\mathbf{k}} \sum_{\mathbf{k}'} W_{\mathbf{k}'} (\beta_{\mathbf{k}'} + \beta_{\mathbf{k}'}^*) \\ & + \frac{g_\Lambda}{2} W_{\mathbf{k}}^{-1} \sum_{\mathbf{k}'} W_{\mathbf{k}'}^{-1} (\beta_{\mathbf{k}'} - \beta_{\mathbf{k}'}^*), \end{aligned} \quad (4)$$

$$\dot{\phi}(t) = g_\Lambda n + \frac{1}{2} g_\Lambda \sqrt{n} \sum_{\mathbf{k}} W_{\mathbf{k}} (\beta_{\mathbf{k}} + \beta_{\mathbf{k}}^*) + \frac{\mathbf{P}^2 - \mathbf{P}_B^2[\beta_{\mathbf{k}}]}{2m_I}.$$

Here $\mathbf{P}_B[\beta_{\mathbf{k}}] = \sum_{\mathbf{k}} \mathbf{k} |\beta_{\mathbf{k}}|^2$ is the total phonon momentum. Here the interaction parameter g_Λ is obtained from the solution of the two-body scattering problem of Eq. (2). The relation between g_Λ and the impurity-boson scattering length a_{IB} is given by the Lippmann-Schwinger equation

$$g_\Lambda^{-1} = \frac{\mu_{\text{red}}}{2\pi} a_{IB}^{-1} - \frac{1}{L^d} \sum_{\mathbf{k}}^\Lambda \frac{2\mu_{\text{red}}}{\mathbf{k}^2}. \quad (5)$$

with the reduced mass of the impurity-boson problem $\mu_{\text{red}} = m_I m_B / (m_I + m_B)$ and the ultraviolet (UV) cutoff

scale $\Lambda \sim 1/r_0$. Note that the UV cut off is related to a finite range r_0 of the interaction potential. In the limit $\Lambda \rightarrow \infty$ the interaction is contact.

II. STATIONARY SOLUTION: POLARON STATE

In this section we derive the saddle point solution of the equations of motions of the parameters in (4). We set the left hand side of the first equation to zero and obtain the following equation which defines the saddle point

$$g_\Lambda \sqrt{n} W_{\mathbf{k}} + \Omega_{\mathbf{k}} [\beta_{\mathbf{k}}] \text{Re} \beta_{\mathbf{k}} + g_\Lambda W_{\mathbf{k}} \sum_{\mathbf{k}'} W_{\mathbf{k}'} \text{Re} \beta_{\mathbf{k}'} = 0 \quad (6)$$

where the dispersion relation

$$\Omega_{\mathbf{k}} [\beta_{\mathbf{k}}] = \omega_{\mathbf{k}} + \frac{\mathbf{k}^2}{2m_I} - \frac{\mathbf{k}(\mathbf{P} - \mathbf{P}_B [\beta_{\mathbf{k}}])}{m_I}. \quad (7)$$

The equation for the imaginary part of the variational parameter always has a trivial solution $\text{Im} \beta_{\mathbf{k}} = 0$. Further we imply that in the stationary state $\beta_{\mathbf{k}}$ is real.

To solve the equation for the real part of $\beta_{\mathbf{k}}$ we rewrite the equation (6) such that we obtain a closed equation for $\chi = \sum_{\mathbf{k}} W_{\mathbf{k}} \beta_{\mathbf{k}}$, $\chi = - \sum_{\mathbf{k}} \frac{g_\Lambda W_{\mathbf{k}}^2}{\Omega_{\mathbf{k}} [\beta_{\mathbf{k}}]} (\sqrt{n_0} + \chi)$. We substitute to the equation of this equation to the expression for $\beta_{\mathbf{k}}$ (6).

$$\beta_{\mathbf{k}} = - \frac{W_{\mathbf{k}}}{\Omega_{\mathbf{k}} [\beta_{\mathbf{k}}]} \frac{2\pi \sqrt{n_0}}{\mu_{\text{red}} (a_{IB}^{-1} - a_*^{-1} [\beta_{\mathbf{k}}])}$$

Here we used the Lipmann-Schwinger equation (5) to regularize the UV divergence in the denominator. We introduce the shift of the Feshbach resonance $\frac{\mu_{\text{red}}}{2\pi} a_*^{-1} [\beta_{\mathbf{k}}] \equiv \sum_{\mathbf{k}}^\Lambda \left(\frac{2\mu_{\text{red}}}{k^2} - \frac{W_{\mathbf{k}}^2}{\Omega_{\mathbf{k}} [\beta_{\mathbf{k}}]} \right)$. Note that this is just a formal solution, where $a_*^{-1} [\beta_{\mathbf{k}}]$ and $\Omega_{\mathbf{k}} [\beta_{\mathbf{k}}]$ are the functional of $\beta_{\mathbf{k}}$.

We substitute the solution for $\beta_{\mathbf{k}}$ to the functionals $\mathbf{P}_B [\beta_{\mathbf{k}}]$ and $a_*^{-1} [\beta_{\mathbf{k}}]$ and obtain two closed integral equations which fully describe the stationary state of the system in the long-time limit

$$\begin{aligned} \mathbf{P}_B &= \frac{4\pi^2 n_0}{\mu_{\text{red}}^2 (a_{IB}^{-1} - a_*^{-1})^2} \sum_{\mathbf{k}} \frac{\mathbf{k} W_{\mathbf{k}}^2}{\left(\omega_{\mathbf{k}} + \frac{\mathbf{k}^2}{2m_I} - \frac{\mathbf{k}}{m_I} (\mathbf{P} - \mathbf{P}_B) \right)^2} \\ a_*^{-1} &= \sum_{\mathbf{k}} \left(\frac{4\pi}{|\mathbf{k}|^2} - \frac{2\pi \mu_{\text{red}}^{-1} W_{\mathbf{k}}^2}{\omega_{\mathbf{k}} + \frac{\mathbf{k}^2}{2m_I} - \frac{\mathbf{k}}{m_I} (\mathbf{P} - \mathbf{P}_B)} \right) \end{aligned} \quad (8)$$

We solve these equations numerically for any given total momentum of the system \mathbf{P} and given interaction a_{IB}^{-1} .

A. Energy of the stationary state

We first calculate the polaron energy $\langle \Psi_{\text{coh}} | \hat{\mathcal{H}} | \Psi_{\text{coh}} \rangle$

$$E_{\text{pol}} = \frac{\mathbf{P}^2 - \mathbf{P}_B^2}{2M} + \frac{2\pi}{\mu_{\text{red}}} \frac{n}{a_{IB}^{-1} - a_*^{-1}}. \quad (9)$$

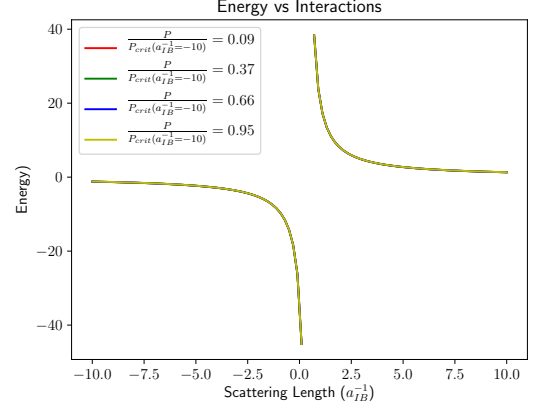


Figure 1. The dependence of energy E_{pol} given by the equation (9) on the inter-species scattering length a_{IB}^{-1} for different total momentum of the system $\mathbf{P} = 0.09, 0.37, 0.66, 0.95 m_I v_s$ where v_s is the speed of sound of the Bose gas $v_s = \sqrt{g_{BB}}$. Here and in the following we fix the bose-bose interaction constant to $g_{BB} = 0.05$, density of the BEC $n = 1$, and mass of the bosons $m_B = m_I = 1$.

The dependence of energy as a function of the inverse impurity-boson scattering length a_{IB}^{-1} is shown in Fig. 1 for different total momentum of the system. The energy of the stationary state is divergent at $a_{IB}^{-1} = a_*^{-1}$. While in fact a_*^{-1} is a function of a total momentum of the system \mathbf{P} the dependence is weak and energy curves for different momenta fall on top of each other (see Fig. 1).

Note, that even for the finite momentum P energy of the system is a UV-convergent quantity. This directly follows from the equation (9) where all entries are fully UV-convergent, a_*^{-1} and \mathbf{P}_B .

The dependence of the energy on the total momentum of the system P for fixed interaction strength a_{IB}^{-1} is shown in Fig. 2. At small momenta the energy spectrum can be approximated with a quadratic function $E(P) \approx E(0) + P^2/2M_P$ where M_P is the effective mass of the polaron. For larger momenta $E(P)$ deviates from the quadratic dependence on the momenta and linear terms become relevant.

B. Polaron mass

We calculate the effective mass by taking the second derivative of the polaron energy with respect to the total momentum $M^* = \left(d^2 E_{\text{pol}} / d|\mathbf{P}|^2 \right)^{-1}$. In practice one can also use the quasi-classical correspondence principle to calculate the effective mass. In the stationary state the velocity carried by the velocity of the impurity, $\mathbf{P}_{\text{imp}}/m_I$, should coincide with the velocity of the polaron, $\mathbf{P}/M_{\text{pol}}$. The momentum of the polaron carried by the impurity is the difference between the total momentum of the system and the momentum carried by the bosons, $\mathbf{P}_{\text{imp}} = \mathbf{P} - \mathbf{P}_{\text{ph}}$. Thus, we obtain the following

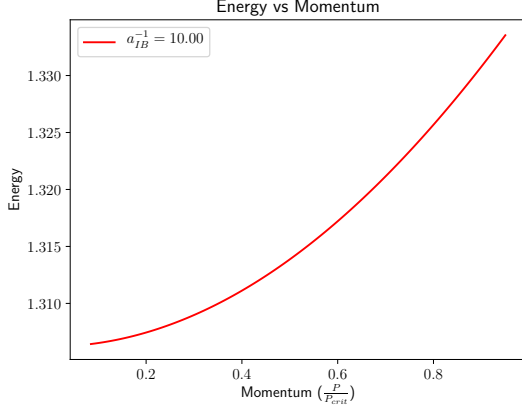


Figure 2. The dependence of energy $E_{\text{pol}}(P)$ given by the equation (9) on the total momentum of the system P/P_{crit} where P_{crit} is defined in Sec. IID.

expression for the effective mass of the polaron

$$\frac{m_I}{M_{\text{pol}}} = 1 - \frac{|\mathbf{P}_B|}{|\mathbf{P}|}. \quad (10)$$

The dependence of the polaron mass is shown in Fig. 3 across the Feshbach resonance. In contrast with the Fröhlich model where mean-field solution gives linear dependence of the effective polaron mass as a function of the interaction. By accounting the two boson scattering terms in the Hamiltonian (1) we demonstrate that even the solution using the coherent states in the polaron frame provides a non-linear dependence for the effective polaron mass as a function of the interacting strength a_{IB}^{-1} . The effective mass diverges as the shifted Feshbach resonance is approached $a_{IB}^{-1} \rightarrow a_*^{-1} \pm 0$. And the effective mass is infinite exactly at the resonance point.

Yulia: What is the power of this divergence? $(a_{IB}^{-1} - a_*^{-1})^\nu$. For the Fröhlich model this divergence is set by the Born approximation. Check if the self-consistency changes the exponent.

C. Number of excitations and Z-factor

The diverging effective mass of the polaron suggest that the number of excitations diverges as well when the shifted Feshbach resonance is approached. The number of bosonic excitations, $N_{\text{pol}} = \sum_{\mathbf{k}} |\beta_{\mathbf{k}}|^2$, is closely related to the quasiparticle residue (Z-factor). The quasiparticle residue is defined as an overlap between the non-interacting state of the system and the polaron state,

$$Z_{\text{pol}} = |\langle 0 | \Psi_{\text{pol}} \rangle|^2 = e^{-N_{\text{pol}}}. \quad (11)$$

In Fig. 4 the dependence of the Z-factor is shown across the inter-species Feshbach resonance for different total momenta of the system. Far away from the resonance, in

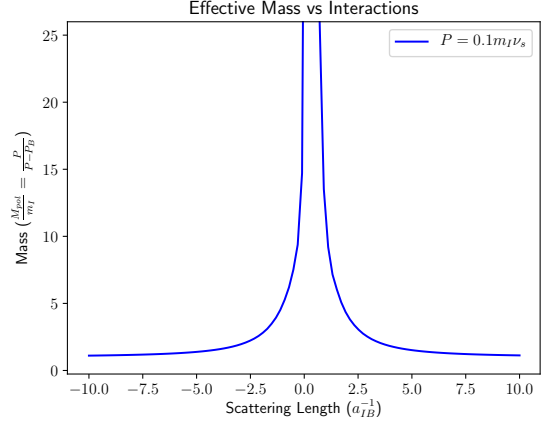


Figure 3. The dependence of polaron mass M_{pol}/m_I given by the equation (10) on the inter-species scattering length a_{IB}^{-1} for different total momentum of the system $\mathbf{P} = 0.1 m_I v_s$.

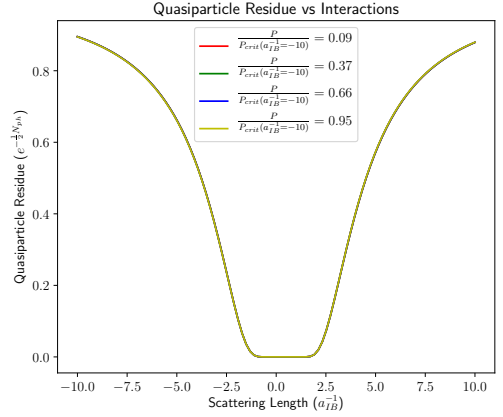


Figure 4. Quasiparticle residue Z_{pol} given by the equation (11) as a function of the inter-species scattering length a_{IB}^{-1} for different total momentum of the system $\mathbf{P} = 0.09, 0.37, 0.66, 0.95 m_I v_s$.

the weakly interacting regime, the quasiparticle residue is of order of unity. Closer to the resonance, both on the repulsive and attractive branches of the polaron state, Z-factor is substantially suppressed. In fact, the dependence of the quasiparticle weight in the interaction strength is exponential, $Z_{\text{pol}} = e^{-\#(a_{IB}^{-1} - a_*^{-1})^{-2}}$. At the shifted resonance Z-factor is exactly equals to zero.

As in the case of the energy, the Z-factor shows very weak dependence on the total momentum of the system all lines in Fig. 4 are fall on top of each other.

D. Impurity momentum

We showed in Fig. 1 and Fig. 4 that energy and Z-factor are insensitive to the change of total momentum of the

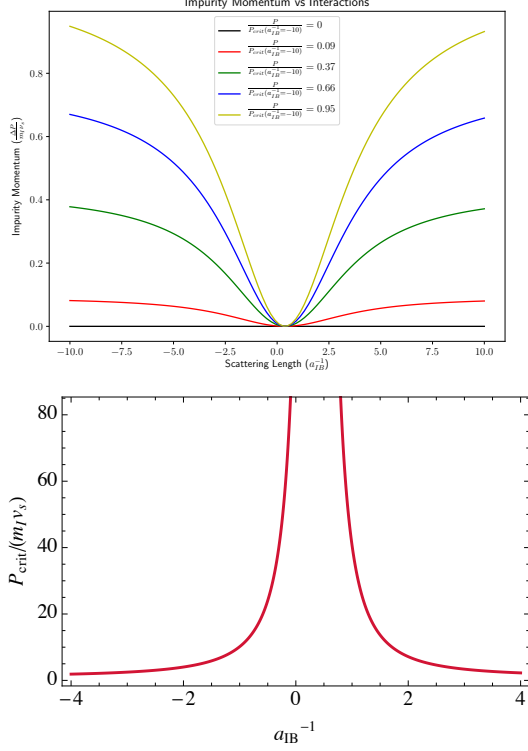


Figure 5. **Top panel:** Impurity momentum $P - P_{\text{ph}}$ in the polaron state as a function of the inter-species scattering length a_{IB}^{-1} for different total momentum of the system $\mathbf{P} = 0.09, 0.37, 0.66, 0.95 m_I v_s$. Close to the Feshbach resonance fraction of the momentum carried by the impurity seems to be decreases rapidly. **Bottom panel:** Critical total momentum P_{crit} as a function of the inter-species scattering length a_{IB}^{-1} .

system within a range of total momentum $P = (0, m_I v_s)$ where v_s is a speed of sound in the BEC. The reason for such weak dependence is hidden in the renormalization of the impurity momentum close to the Feshbach resonance. Fig. 5 shows the impurity momentum $P - P_{\text{ph}}$ as a function of the inter-species strength close to the resonance. As we can see from this figure even starting from a relatively large total momentum of the system $\sim m_I v_s$ close to the Feshbach resonance impurity does not acquire any momentum. This is consistent with our calculation of the impurity mass renormalization, near the resonance the effective mass of the polaron is divergent (see Fig. 3). This means that even when total momentum of the system is large impurity's velocity is very small in comparison with the sound velocity in the BEC. That suggest strong renormalization of the critical total momentum as a function of interaction strength.

We define the critical total momentum of the system using equation (8) where we fix the impurity velocity equal to the speed of sound in the BEC, $P_I = \mathbf{P} - \mathbf{P}_B =$

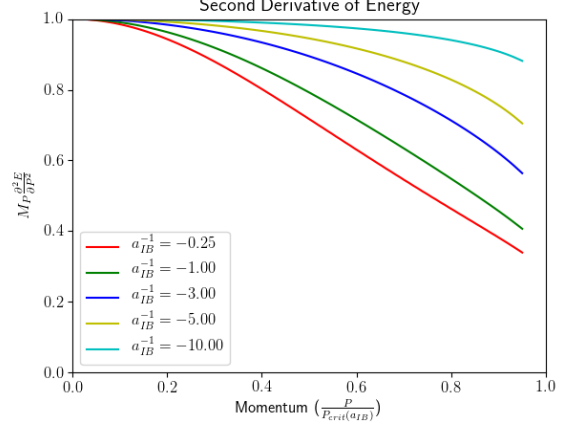


Figure 6. Comparison between the spectrum's curvature $\partial^2 E(P)/\partial P^2$ and the effective mass of the polaron in the $P \rightarrow 0$ limit. The plot demonstrates the product of two, $M_{\text{pol}} \partial^2 E(P)/\partial P^2$, as a function of critical momenta P_{crit} for different interaction strength a_{IB}^{-1} on the negative side of the Feshbach resonance.

$m_I v_s$,

$$\mathbf{P}_{B,\text{crit}} = \frac{4\pi^2 n_0}{\mu_{\text{red}}^2 (a_{IB}^{-1} - a_*^{-1})^2} \sum_{\mathbf{k}} \frac{\mathbf{k} W_{\mathbf{k}}^2}{\left(\omega_{\mathbf{k}} + \frac{\mathbf{k}^2}{2m_I} - k v_s \cos \theta \right)^2}$$

$$a_*^{-1} = \sum_{\mathbf{k}} \left(\frac{4\pi}{|\mathbf{k}|^2} - \frac{2\pi \mu_{\text{red}}^{-1} W_{\mathbf{k}}^2}{\omega_{\mathbf{k}} + \frac{\mathbf{k}^2}{2m_I} - k v_s \cos \theta} \right) \quad (12)$$

Here a_*^{-1} is a number which depends on the bose-bose interaction strength g_{BB} and the dependence on a_{IB}^{-1} is only due to the prefator in the equation for \mathbf{P}_B . Thus, the critical total momentum $P_{\text{crit}} = P_{B,\text{crit}} + m_I v_s$ divergent at $a_{IB}^{-1} = a_*^{-1}$ as $(a_{IB}^{-1} - a_*^{-1})^{-2}$.

E. Spectrum curvature vs polaron mass

We compare the spectrum curvature $\partial^2 E(P)/\partial P^2$ with the inverse effective polaron mass M_{pol}^{-1} calculated in Sec. II B. Fig. 6 shows that the second derivative of the energy changes significantly as the critical momentum is approached. This effect is more pronounced close to the Feshbach resonance.

F. Full counting statistics of the impurity momentum

We derive the momentum distribution function for the single impurity in a BEC. In the polaron (LLP) frame, the wavefunction is $|\psi_{\text{pol}}\rangle = e^{\sum_{\mathbf{k}} \beta_{\mathbf{k}} b_{\mathbf{k}}^\dagger - \sum_{\mathbf{k}} \beta_{\mathbf{k}}^* b_{\mathbf{k}}} |0\rangle = |\beta\rangle$. We get the wavefunction in the laboratory frame by doing an inverse LLP transformation. As we initially transformed the Hamiltonian as $\mathcal{H} \rightarrow \hat{U}_{LLP}^\dagger \mathcal{H} \hat{U}_{LLP}$ with

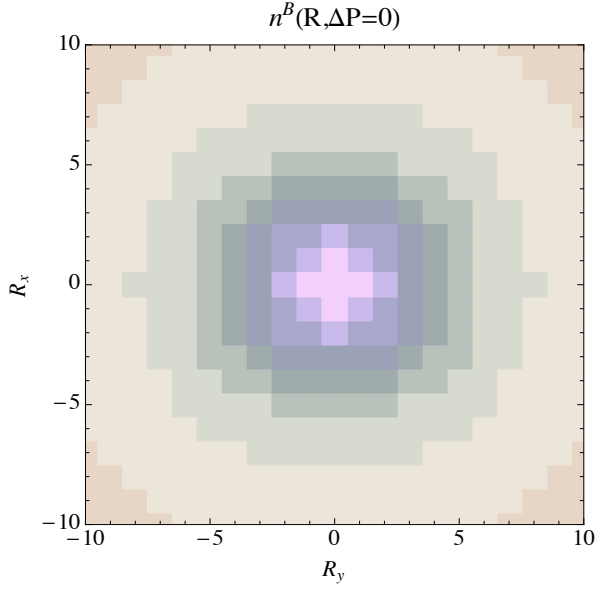


Figure 7. Distribution of the density of bosonic excitations in real space for $P = 0$.

$\hat{U}_{LLP} = e^{-i\hat{R}_I \sum_k k \cdot b_k^\dagger b_k}$, we have $|\psi_{pol}\rangle = \hat{U}_{LLP}^\dagger |\psi(R_I)\rangle$. Therefore, we have:

$$|\psi(R_I)\rangle = \hat{U}_{LLP} |\psi_{pol}\rangle = e^{-i\hat{R}_I \sum_k k \cdot b_k^\dagger b_k} |\psi_{pol}\rangle \quad (13)$$

The impurity's momentum distribution function is given by the projection of the wavefunction of the system into the subspace of impurity momentum $\hat{n}_Q^I = |Q\rangle\langle Q|$

$$\begin{aligned} n_Q^I &= \langle \psi_{pol} | U_{LLP}^{-1} | Q \rangle \langle Q | U_{LLP} | \psi_{pol} \rangle \\ &= \int dR dR' \langle \psi_{pol} | U_{LLP}^{-1} | R \rangle e^{i(R-R')Q} \langle R' | U_{LLP} | \psi_{pol} \rangle \\ &= \int d\rho e^{i\rho Q} \langle \psi_{pol} | e^{-i\rho \sum_k k \cdot b_k^\dagger b_k} | \psi_{pol} \rangle \end{aligned} \quad (14)$$

Thus, we can define the impurity momentum distribution function as a Fourier transform of the expectation value of the generating function $e^{-i\rho \sum_k k \cdot b_k^\dagger b_k}$. Averaging this operator with the coherent state we obtain

$$n_Q^I = \int d\rho e^{i\rho Q} e^{\sum_k |\beta_k|^2 (e^{-i k \rho} - 1)} \quad (15)$$

Notice that the momentum distribution of the impurity is closely related to the distribution function of the bosons in the polaron frame which is given by $n_k^B = |\beta_k|^2$.

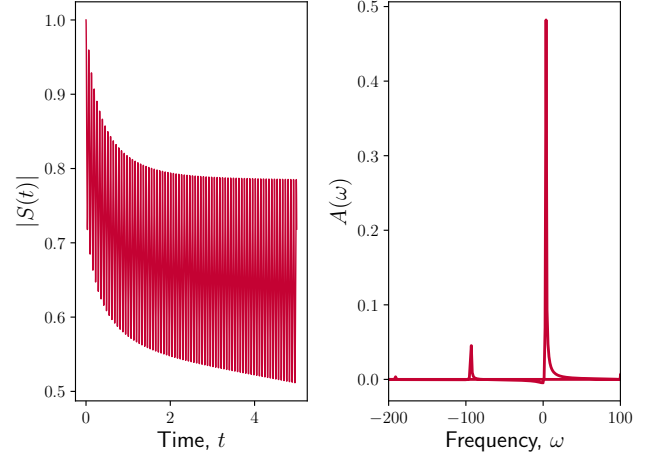


Figure 8. Dynamical overlap $|S(t)|$ (left panel) and the spectral function $A(\omega)$ (right panel) of the repulsive polaron $a_{IB}^{-1} = 5$. Time evolution of $|S(t)|$ shows rapid oscillations which are due to the formation of the bound states. These bound states are resolved in the spectral function in the right panel. For the numerical calculations we use $\Lambda = 20$.

G. Time-of-flight measurement

III. DYNAMICS OF THE IMPURITY WITH FIXED FINITE MOMENTUM

A. Excitation spectrum

We are interested in the excitation spectrum of the system as a function of its total momentum. In experiments the spectrum can be explored using ‘inverse’ RF spectroscopy where the impurity is driven from a state non-interacting with the BEC to an interacting one. Within linear response the absorption spectrum is given by

$$A(\omega) = 2 \operatorname{Re} \int_0^\infty dt e^{i\omega t} S(t), \quad (16)$$

where $S(t) = \langle \Psi(0) | e^{-i\hat{H}t} | \Psi(0) \rangle$ is a dynamical overlap. Here $|\Psi(0)\rangle$ denotes the initial state of the system and the overlap $S(t)$ describes the dynamics of the system after a quench of the between impurity and the bath. In real-time the overlap $S(t)$ can be measured using Ramsey interferometry [? ?]. In the class of coherent states (3) the dynamical overlap is given by

$$S(t) = e^{-i\phi(t)} e^{-\frac{1}{2} N_{ph}} \quad (17)$$

On the attractive side, $a_{IB}^{-1} < 0$, the dynamical overlap is a monotonically decaying function which in the long time limit reaches its equilibrium value which corresponds to the quasiparticle weight Z . The spectral function $A(\omega)$ shows one sharp peak with the position of the peak that corresponds to the energy of the polaron $E_{pol} < 0$. The spectrum is overall is very similar to the spectrum of the impurity with $P = 0$.

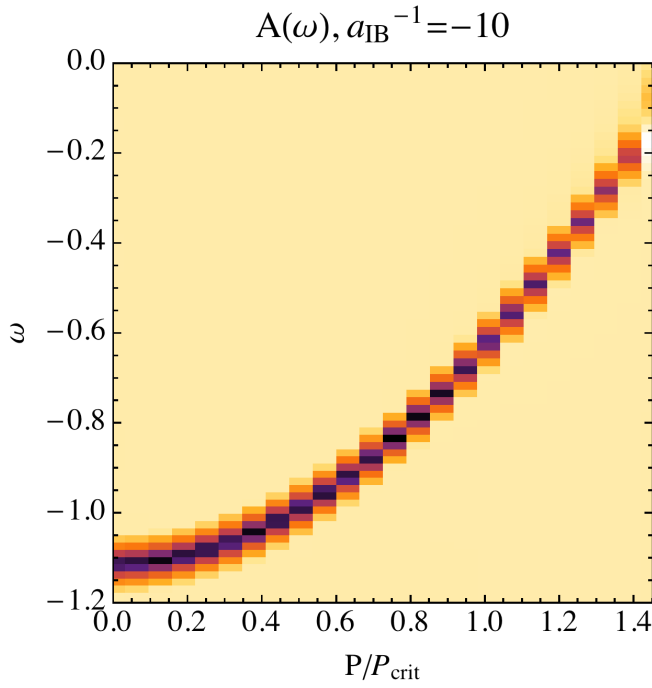


Figure 9.

On the repulsive side, $a_{IB}^{-1} > 0$, the dynamical overlap is a rapidly oscillating function (i.e. see Fig. 8). These oscillations are the consequences of the multi-particle bound states formation process. In the Fourier transform of the $S(t)$ these bound states are well resolved and forms an equidistant spectrum.

B. Subsonic-supersonic transition

C. (Anomalous) diffusion

Yulia: Calculate $x^2(t)$ and figure out if it is normal or anomalous diffusion.

To calculate the

IV. DYNAMICS OF THE RELEASED IMPURITY

Yulia: Derive some expressions for the properties of impurities in real time after being released from the trapping potential.

Consider several trapping geometries

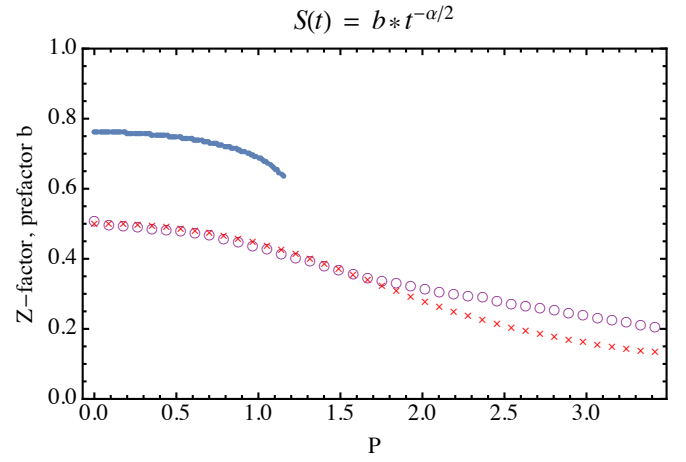


Figure 10.

A. Harmonic oscillator trap

B. Pancake geometry

V. DISCUSSION WITH MISHA

TO DO LIST:

1. Z-factor is the same for $S(t)$ and n_k
2. Check Z-factor of a static problem and dynamic problem is the same.
3. $\langle \Psi_{\text{pol}} | P_{\text{imp}} | \Psi_{\text{pol}} \rangle \neq \lim_{t \rightarrow \text{inf}} \langle \Psi(t) | P_{\text{imp}} | \Psi(t) \rangle$
4. Check $n_{\text{imp}}^{\text{pol}} = \lim_{t \rightarrow \text{inf}} n_{\text{imp}}(t)$